

available at www.sciencedirect.comjournal homepage: www.elsevier.com/locate/diinDigital
Investigation

Classification of digital camera-models based on demosaicing artifacts

Sevinc Bayram^{a,*}, Husrev T. Sencar^b, Nasir Memon^b^aDepartment of Electrical and Computer Engineering, Polytechnic University, Brooklyn, NY, USA^bDepartment of Computer and Information Science, Polytechnic University, Brooklyn, NY, USA

ARTICLE INFO

Article history:

Received 7 November 2007

Received in revised form

16 April 2008

Accepted 7 June 2008

Published online ■

Keywords:

Image forensics

Source identification

Demosaicing

Camera

Camera-model

Color filter array

ABSTRACT

We utilize traces of demosaicing operation in digital cameras to identify the source camera-model of a digital image. To identify demosaicing artifacts associated with different camera-models, we employ two methods and define a set of image characteristics which are used as features in designing classifiers that distinguish between digital camera-models. The first method tries to estimate demosaicing parameters assuming linear model while the second one extracts periodicity features to detect simple forms of demosaicing. To determine the reliability of the designated image features in differentiating the source camera-model, we consider both images taken under similar settings at fixed sceneries and images taken under independent conditions. In order to show how to use these methods as a forensics tool, we consider several scenarios where we try to (i) determine which camera-model was used to capture a given image among three, four, and five camera-models, (ii) decide whether or not a given image was taken by a particular camera-model among very large number of camera-models (in the order of hundreds), and (iii) more reliably identify the individual camera, that captured a given image, by incorporating demosaicing artifacts with noise characteristics of the imaging sensor of the camera.

© 2008 Elsevier Ltd. All rights reserved.

1. Introduction

Digital imagery is becoming an integral part of our daily lives at a rapid pace. As a result of this shift in technology, conventional film photography is disappearing. When combined with the availability of extremely powerful image processing techniques and computer graphics technologies, this trend poses new issues and challenges concerning the accountability of digital images. This problem is further exacerbated when photographic evidence is considered. Digital image forensics techniques aim at closing this gap by uncovering facts about a digital image (Sencar and Memon, 2008; Tran Van Lanh et al., 2007; Ng et al., 2006). In deciding the authenticity and admissibility of a digital image, we face three

important problems. First is the identification of how an image is generated. Most research effort in this area has focused on discriminating computer generated images, which does not depict real-life occurrences, from real images (Dehnie et al., 2006; Dirik et al., 2007; Tian-Tsong, 2005; Wang and Moulin, 2006). Second problem deals with determining whether or not an image has undergone any form of modification or processing after it was initially captured. Many techniques for detecting image forgeries are proposed for this purpose (Swaminathan et al., 2006; Bayram et al., October–December 2006; Johnson and Farid, 2005; Popescu and Farid, 2005, 2004). The other key problem in image forensics is identification and analysis of image characteristics that relate to the acquisition device. Due to prevalence of digital cameras, Q1

* Corresponding author.

E-mail addresses: sevinc@isis.poly.edu (S. Bayram), taha@isis.poly.edu (H.T. Sencar), memon@poly.edu (N. Memon).

1742-2876/\$ – see front matter © 2008 Elsevier Ltd. All rights reserved.

doi:10.1016/j.diin.2008.06.004

115 in this area, research efforts have focused primarily on design
116 of techniques to determine the source camera and camera-
117 model of an image.

118 In this paper, we focus on the image source identification
119 problem where the goal is to obtain information on the digital
120 camera used in capturing of a given image. This is realized by
121 analyzing images and extracting characteristics that relate to
122 source digital camera. These characteristics are essentially
123 a combination of two interrelated factors: first, the class
124 properties that are common among all cameras of a brand and
125 model; and second, the individual properties that sets a camera
126 apart from another in its class. Hence, the approaches in this
127 field can be categorized into two based on whether proposed
128 techniques aim at identifying class or individual properties of
129 the digital camera used in capturing the image as described
130 below.

- 131 • The first approach in this area tries to detect the source
132 camera-model of the image by determining the differences
133 in image formation pipeline, e.g., processing techniques and
134 component technologies. For this purpose, [Kharrazi et al.](#)
135 [\(2004\)](#) utilized a set of image features which includes color
136 characteristics, image quality metrics, and wavelet coeffi-
137 cient statistics, [Choi et al. \(2006\)](#) considered optical
138 distortions due to a type of lens and incorporated it with the
139 features of [Kharrazi et al. \(2004\)](#), and [Swaminathan et al.](#)
140 [\(2007\)](#) and [Long and Huang \(2006\)](#) explored the differences
141 due to choice of color filter array and the corresponding
142 demosaicing algorithm. The main difficulty with camera-
143 model identification is that many camera-models and
144 brands use components by a few manufacturers, and
145 processing methods remain same or very similar among
146 different models of a brand. Hence, reliable identification of
147 class characteristics of a camera requires consideration of
148 many different factors.
- 149 • In the second approach, the goal is to identify unique char-
150 acteristics of the source camera. These characteristics may
151 be in the form of hardware and component imperfections,
152 defects, or faults which might arise due to inhomogeneity in
153 the manufacturing process, manufacturing tolerances,
154 environmental effects, and operating conditions. The ability
155 to reliably extract these characteristics makes it possible to
156 match an image to its potential source and cluster data from
157 the same source camera together. For this purpose, in
158 [Kurosawa et al. \(1999\)](#) fixed pattern noise caused by dark
159 currents in (video camera) imaging sensors is detected, and
160 in [Geradts et al. \(2001\)](#) using traces of defective pixels, e.g.,
161 hot pixels, cold/dead pixels, pixel traps, cluster defects is
162 proposed, in [Dirik et al. \(April 2007\)](#) authors took the
163 advantage of unique dust specks on the lens which are
164 mostly imperceptible artifacts in images and in [Lukáš et al.](#)
165 [\(2006\)](#) and [Chen et al. \(2007, February 2007\)](#) sensor noise of
166 the image is used for identifying the source of the image. The
167 main challenge in this research direction is that reliable
168 measurement of these minute differences from a single
169 image is difficult and can be easily eclipsed by the image
170 content itself. Another challenge is that these artifacts tend
171 to vary in time and depend on operating conditions; there-
fore, they may not always yield positive identification.

172 In this paper, we describe our approaches to identify,
173 detect and classify traces of demosaicing operation. Most
174 state-of-the art digital cameras employ a single color filter
175 array (CFA) rather than having different filters for each color
176 band to generate color images. As a result of using a single
177 CFA, each pixel is only represented by single color value and
178 an interpolation operation has been performed to obtain the
179 missing color values at each pixel operation. Therefore,
180 demosaicing is a common processing technique that is
181 central to operation of most digital cameras. Due to its
182 proprietary design and implementation, the choice of CFA
183 and demosaicing operation provides a unique opportunity
184 to determine the source camera-model of a given digital
185 image.

186 In our initial approach ([Bayram et al., 2005](#)), we aimed at
187 detecting artifacts due to color interpolation. Our approach
188 was inspired by the technique proposed by [Popescu and](#)
189 [Farid \(2004\)](#) which introduced statistical measures to detect
190 image up-sampling operation for the purpose of detecting
191 image tampering. We have applied variants of such
192 measures to characterize the specifics of the deployed
193 interpolation algorithm. Later, in [Bayram et al. \(2006\)](#) we
194 improved our approach based on the premise that most
195 proprietary algorithms in smooth image parts will deploy
196 simpler forms of interpolation, and therefore, they can be
197 captured more effectively (as opposed to busy image parts
198 where interpolation requires more careful processing). For
199 this purpose, we utilized the results of [Gallagher et al. \(2005\)](#)
200 where the characteristics of the second-order derivative of
201 interpolated signals are analyzed. More specifically in this
202 paper, the features considered in [Bayram et al. \(2005, 2006\)](#)
203 are combined and tested with image-sets acquired under
204 both similar circumstances and independently. Results
205 obtained for up to five digital camera-models show the
206 success of the proposed approach. We further extend our
207 approach to the case where a single camera-model is
208 discriminated from a very large number of digital camera-
209 models. We also describe and demonstrate how camera-
210 model identification methods can be used to complement
211 individual source identification methods to provide more
212 reliable identification results ([Sutcu et al., 2007](#)). For this
213 purpose, we incorporate our approach with the technique
214 proposed in [Lukáš et al. \(2006\)](#). In this method, a determin-
215 istic component of imaging sensor noise is extracted from
216 a set of images as a fingerprint of a digital camera. Later,
217 through use of correlative procedures the presence of the
218 extracted noise pattern in a given image is used to decide the
219 source camera of an image. To further improve the results of
220 [Lukáš et al. \(2006\)](#) (in terms of reducing false-positives), we
221 include model properties of the camera as another layer of
222 verification.

223 The rest of this paper is organized as follows: In Section 2,
224 we briefly describe the image formation process in digital
225 cameras. Details of our approach to source camera-model
226 identification by detecting traces of demosaicing operation are
227 provided in Section 3. In Section 4, we present a composite
228 method to more reliably identify the individual source
camera. We provide our experimental results in Section 5 and
conclude in Section 6.

2. Demosaicing and image formation in digital cameras

The basic architecture and sequence of processing steps remain very similar in all digital cameras (despite the proprietary nature of the underlying technology). The basic structure of image formation pipeline in digital cameras can be illustrated as given in Fig. 1. In a digital camera, the light entering the camera through the lens is first filtered (the most important being an anti-aliasing filter) and focused onto an array of charge-coupled device (CCD) elements, i.e., pixels. The CCD array is the main and most expensive component of a digital camera. Each light sensing element of CCD array integrates the incident light over the whole spectrum and obtains an electric signal representation of the scenery. Since each CCD element is essentially monochromatic, capturing color images requires separate CCD arrays for each color component. However, due to cost considerations, in most digital cameras, only a single CCD array is used by arranging them in a pattern where each element has a different spectral filter, typically one of red, green or blue (RGB). This mask in front of the sensor and it is called the color filter array (CFA). Consequently, each CCD element only senses one band of wave-lengths, and the raw image collected from the array is a mosaic of red, green and blue pixels. Since human visual system is more sensitive to green light, CFA patterns typically have more green values than red and blue. Fig. 2 displays two common CFA patterns used in RGB and CMYK color spaces.

As a result of the use of a CFA, each pixel in the image has only one color component associated with it. The missing RGB values are calculated based on the neighboring pixels values by an operation called *demosaicing*. Demosaicing is essentially a form of interpolation which is carried out by *properly* weighting and combining the color values of pixels selected within a window around the missing value. In practice, interpolation operation is defined by the size of the window

and how the weighting coefficients are determined (interpolation kernel). Although each manufacturer uses proprietary methods, i.e., kernels with different sizes, shapes and different interpolation algorithms, demosaicing techniques can be grouped in two-classes. The first class includes well-known interpolation techniques such as nearest neighborhood, bilinear and bi-cubic interpolation. These techniques treat all color channels as three independent images and basically just use the neighbor pixels with different interpolation kernels to calculate the missing color component. In smooth regions of an image, these single-channel algorithms can provide satisfactory results but they usually fail in high frequency regions, especially along the edges and leave heavy interpolation artifacts. Better performance can be achieved using the fact that three color channels are highly correlated to each other. The second class of algorithms uses these inter-channel correlations in addition to in-channel interpolations, e.g., edge directed interpolation, constant hue-based interpolation, second-order gradients, alias canceling interpolation, homogeneity directed interpolation, pattern matching, vector based interpolation, Fourier based filtering, etc. A survey of the second class algorithms can be found in Gunturk et al. (2004).

After demosaicing, white balancing operation is performed which is basically the process of removing unrealistic color casts, so that objects which appear white in human visual system are rendered white in the digital image. This is followed by colorimetric interpretation, and gamma correction. Gamma correction is necessary to redistribute tonal information to more closely correspond to the way the human eye perceives brightness since digital cameras perceive light in a linear fashion but human visual system perceives light in logarithmic fashion. After these, noise reduction, anti-aliasing and sharpening are performed to avoid color artifacts. At the end the image is compressed and saved in the memory.

Despite the similarity in their architectures, the processing details at all stages vary widely from one manufacturer to

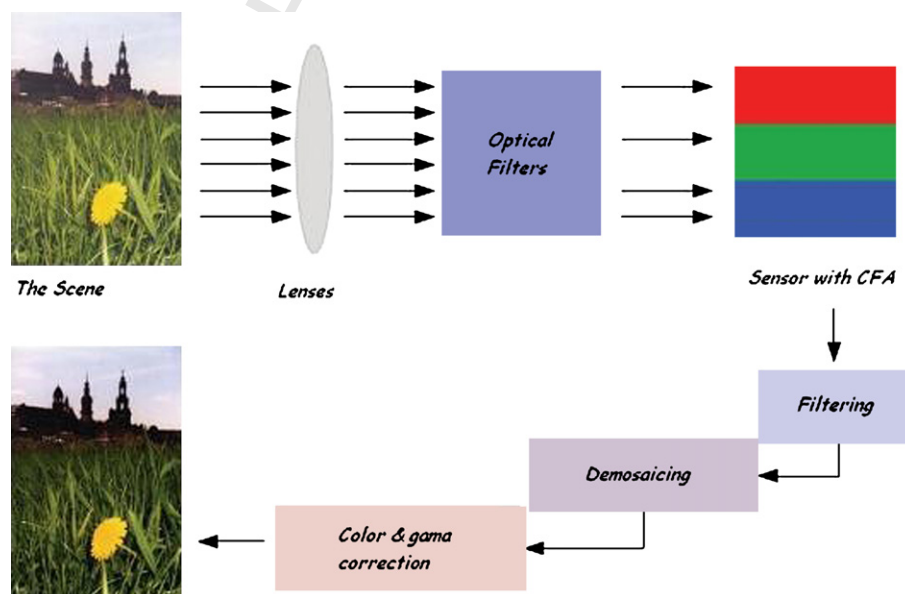


Fig. 1 – The more important stages of camera pipeline.

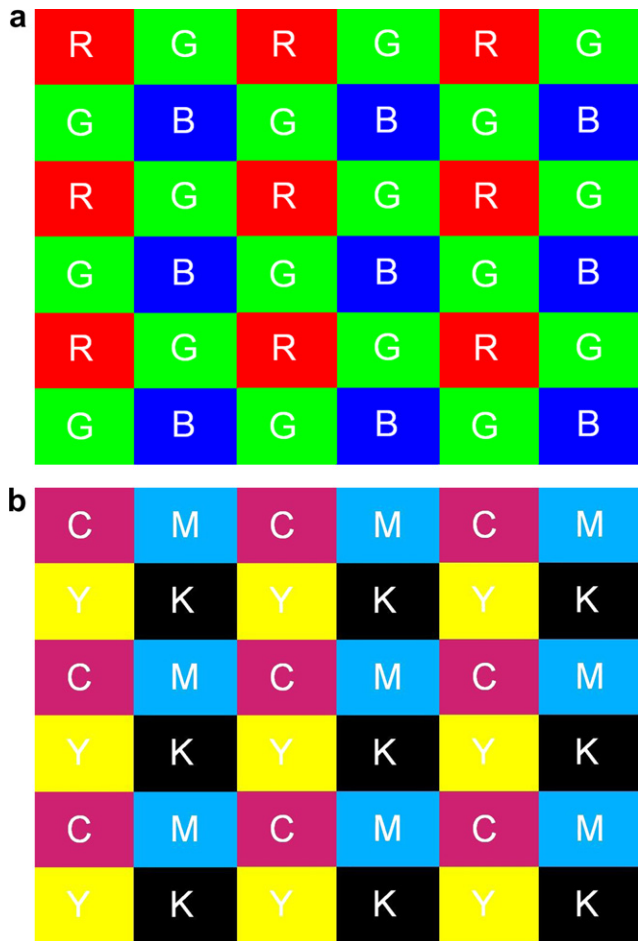


Fig. 2 – (a) CFA pattern using RGB values. (b) CFA pattern using CMYK values.

other, and even in different camera-models produced by the same manufactures. It should also be noted that many components in the image formation pipeline of various digital cameras, (*e.g.*, lens, optical filters, CCD array) are produced by a limited number of manufactures. Due to this overlap, different cameras may exhibit similar qualities, and this should be taken into consideration in associating image features with the properties of digital cameras. However, interpolation (demosaicing) algorithm and the design of the CFA pattern remain proprietary to each digital camera-model, and the variations in the interpolated pixel values can be exploited to classify the images as originating from a certain class of digital cameras.

3. Identifying traces of interpolation

Images taken by digital cameras with a single CCD sensor are evidently interpolated using the CFA and the designated demosaicing algorithms. These algorithms are fine-tuned to prevent visual artifacts, in forms of over-smoothed edges or poor color transitions, in busy parts of the images. Therefore, they are highly non-linear and strongly dependent on the

nature of the depicted scenery. On the other hand, in relatively smooth parts of the image, these algorithms exhibit a rather linear characteristic. As a result, interpolation operation is less likely to depend on the nature of the captured content. Thus, in our analysis we primarily focus on image parts that do not exhibit significant spatial variation.

The interpolation algorithm, used to estimate the missing color values, introduces correlation between neighbor pixels. Since CFA patterns are typically periodic these correlations will be periodic as well. For example consider the Bayer pattern shown in Fig. 2a. To calculate the missing green values over the red and blue values we can basically use bi-cubic interpolation which is just averaging of four nearest neighbors. In this case, one out of two pixels will be correlated to its neighbor pixels with the same weights of 0.25 and the interpolation kernel will be 3×3 . In our approach we start assuming that each pixel value is correlated to its neighbors with the associated weighting coefficients and each camera manufacturer uses different interpolation kernel and/or different weighting coefficients. The crux of our approach lies on estimating these coefficients and associating them with the digital camera-model used to capture the images.

To detect and classify the traces of interpolation operation in images we rely on two methods. The first method is based on the use of Expectation–Maximization algorithm which analyzes the correlation of each pixel value to its neighbors (Popescu and Farid, 2004). The second method is based on analyzing inter-pixel differences (Gallagher et al., 2005). Among the two methods, the former one can be also applied to less smooth parts of the image where the variation is not significant. On the other hand the latter is better suited for extremely smooth parts of the image where a simpler form of interpolation is deployed. In our analysis, we partition the image into blocks based on the level of smoothness decided using relative deviation of the variance in each block.

3.1. Use of Expectation–Maximization algorithm

The Expectation/Maximization (EM) algorithm consists of two major steps: an expectation step, followed by a maximization step (Moon, 1996). The expectation is with respect to the unknown variables, using the current estimate of the parameters, and conditioned upon the observations. The maximization step then provides a new estimate of the parameters. These two steps are iterated until convergence. The EM algorithm generates two outputs. One is a two-dimensional data array, called probability map, in which each entry indicate the similarity of each image pixel to one of the two groups of samples, namely, the ones correlated to their neighbors and those ones that are not, in a selected kernel. The other output is the estimate of the weighting (interpolation) coefficients which designate the amount of contribution from each pixel in the interpolation kernel.

Since color filter arrays have more green color values, the red and blue color channels are more heavily interpolated. Therefore, we employed EM algorithm only on red channel; however, it can be trivially extended to other channels. Since no a priori information is assumed on the size of interpolation kernel probability maps and weighting coefficients are obtained for varying sizes of kernels. Let $p(i, j)$ denote the pixel

value for a selected color channel. We assume this pixel value is correlated to its neighbors by given equation:

$$p(i, j) = \sum_{n, m=-N}^N \beta(n, m) \times p(i - n, j - m) \quad (3.1)$$

In this equation N shows the interpolation kernel size and we denote the weighting coefficient matrix by β . In the expectation step first we assume a random β matrix and using this matrix we calculate the probability of each pixel correlated to its neighbors. In the maximization step we estimate new β parameters according to the probability calculated in the expectation step. We execute these steps iteratively until the convergence of β . When designing our classifiers, we use these β parameters (weighting coefficients) as features.

In our earlier work (Bayram et al., 2005), we extracted features assuming different sizes of interpolation kernels of sizes 3×3 , 4×4 and 5×5 which were subsequently used to design classifiers in distinguishing camera-models. Experimental results showed that the accuracy improves with the increasing kernel sizes. Therefore, in this paper, we assume 5×5 interpolation kernel. Hence, the EM algorithm is used to estimate the weighting coefficients in 5×5 neighborhoods.

3.2. Use of second-order derivatives

Low-order interpolation introduces periodicity in the variance of the second-order derivative of an interpolated signal which can be used to determine the rate of interpolation (Gallagher et al., 2005). In this regard, the method first obtains the second-order derivative of each row and averages it over all rows. To better clarify, let $r(i, \cdot)$ denote a row of the image, and let R be the number of rows and C be the number of columns. The second-order derivative of each row can be computed as follows:

$$sd_r = 2r(i, j) - r(i, j + 1) + r(i, j - 1) \quad (3.2)$$

where $1 \leq j < C - 1$. After obtaining the second-order derivatives of each row, the magnitudes of these rows are averaged together to form a pseudo-variance signal.

$$v_r = \sum_{i=0}^R |s_r(i, j)| \quad (3.3)$$

If the image is interpolated, this pseudo-variance signal exhibits a periodicity. When observed in the frequency domain the locations of the peaks of the variance signal reveal the interpolation rate and the magnitude of the peaks determine the interpolation method. We employed a similar methodology to characterize the interpolation rate and the method employed by a digital camera.

Most digital cameras encode and compress images in JPEG format. Due to 8×8 block coding in JPEG, the DC coefficients may also introduce peaks in the second-order derivative implying the presence of some form of interpolation operation at a rate of 8. Therefore, in detecting the interpolation algorithm, the peaks due to JPEG compression have to be ignored. The variation in magnitude indicates that there are differences in the deployed interpolation algorithm. Fig. 3 displays the magnitude frequency response for the three models of digital cameras. The variation in magnitude indicates that there are differences in the deployed interpolation algorithm.

Therefore, the features extracted from each camera include the location of the peaks (except for the ones due to JPEG compression), their magnitudes, and the energy of each frequency component with respect to other frequency components at all color bands.

In Bayram et al. (2006), we showed that combining features which are extracted using second-order derivative method and EM algorithm improves the performance. Based on this, in this work, instead of designing classifiers for each set of features we design our classifiers for the joint feature set of 78 features in total.

4. Combining demosaicing characteristics with sensor noise properties for individual camera identification

In this section, we describe how extracted class properties (i.e., source camera-model characteristics) can be utilized to more reliably detect the individual source camera of an image. The underlying idea of our approach is that the class properties of the camera extracted from the image needs to be also in agreement with those of the individual camera. Hence, the two types of methods can be combined to more accurately detect source camera of an image.

Lukáš et al. (2006) proposed a procedure to extract one of major components of the sensor pattern noise, namely photo response non-uniformity (PRNU) noise. This method denoises the image by a wavelet based denoising algorithm so that the resulting noise residue contains the needed noise components. However, the resulting residue signal also contains contributions from the image itself. Therefore, to further strengthen the noise pattern and to suppress the random contributions from the image, noise residues obtained from multiple images are averaged together to estimate the source camera's noise pattern, i.e., reference pattern. To identify the source of a given image, the noise residue of the image is correlated with the reference noise patterns extracted from the camera and a decision is made by comparing the measured correlation statistics to pre-determined decision threshold. In Lukáš et al. (2006), reported results obtained from (high quality) images taken by nine cameras show that an identification accuracy of 100% can be achieved.

In our earlier work (Sutcu et al., 2007), using this method we performed experiments under a more realistic setting on an image set with roughly 80,000 randomly selected images to determine the achievable false-positive and true detection performances. We observed that some of the tested cameras yield false-positive rates much higher than the expected values. To reduce this type of errors, we propose to improve the performance of sensor noise extraction based method by also verifying the consistency of demosaicing artifacts, as described in Section 3. Fig. 4 shows a block diagram of the combined method where two methods are used in a sequence. Accordingly, first we use sensor noise based method to test if the image is taken by the individual camera or not. If the decision is positive we further examine whether the image exhibits the traces of demosaicing artifacts of the same camera-model. Therefore in the experiments, at first positive decisions due to sensor noise matching are determined. Then,

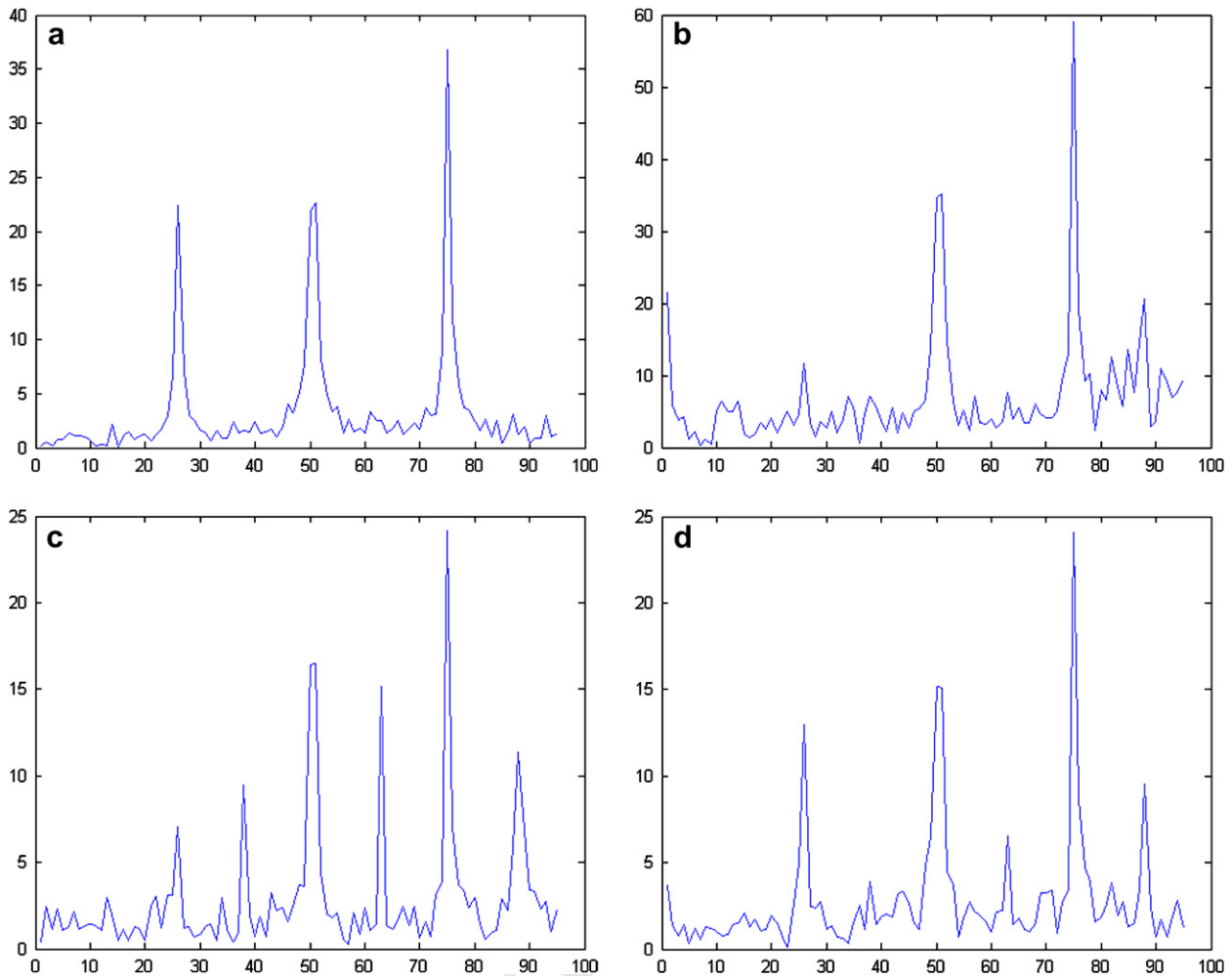


Fig. 3 – Frequency spectrum of averaged second-order derivatives corresponding to JPEG compression and the three models of digital cameras with JPEG output images. (a) Peaks due to JPEG compression (b) Canon Powershot S200 (c) Sony DSC-51 (d) Nikon E-2100.

these images are feed to the classifier to verify the consistency of demosaicing artifacts. Hence, the final decision is made by the classifier. It is expected that the use of combined method would eliminate some of the false-positives due to mismatch of the reference pattern. However, it should be noted that, this procedure may eliminate some of the true positives as well. Therefore, we should make sure that the decrease in false-positive rate can compensate for the decrease in the true positive rate.

In our experiments, we obtained sensor noise patterns of each camera by averaging the noise residues of many (in this work 300) images as described in Lukáš et al. (2006). We collected 600 images from each of three test camera where 300

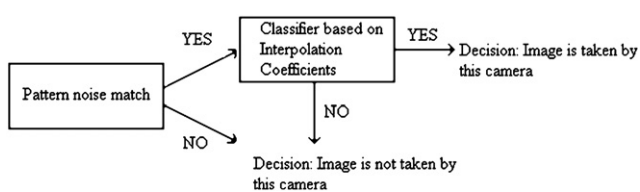


Fig. 4 – The proposed combined method.

of the images were used to obtain a reference pattern and the rest for testing purposes. We also collected 5300 images from various different cameras to test the reliability of only matching the sensors' pattern noise. We performed experiments first just by using sensor noise with various threshold values and later on by the proposed combined scheme.

5. Experiments

We divide our experiments into two categories. The first category of experiments is performed to assess the accuracy of camera-model identification method and the second category of experiments evaluates the improvement in the accuracy of individual camera identification method by incorporating it with described camera-model identification method. In the first category, to test the effectiveness of the proposed features, we performed three sets of experiments. The first set involves images obtained by subsequently photographing the same scenery under similar settings with different camera-models. In the second set, images are taken by cameras

with no prior constraint on the scenery and the acquisition settings. In the third set of the experiments we reduce the problem to a two-class classification problem to decide whether an image is taken by a particular digital camera-model or not. In the second category, we evaluate the improvements in the performance due to incorporation of sensor noise based method of Lukáš et al. (2006) with the proposed camera-model identification method. In our experiments, we used a publicly available support vector machine based classifier as described in Section 5.1. In addition, we used sequential forward floating search (SFFS) (Gallagher et al., 2005) algorithm to reduce the dimensionality of the feature vector by selecting the most distinguishing features. SFFS procedure is explained in Section 5.2.

5.1. SVM classifier

SVMs are based on the idea of minimizing training set error by constructing a hyperplane as the decision surface in such a way that the margin of separation between different classes are maximized. Consider a two-class classification problem with linearly separable data and training feature sets $[m_i, y_i]$ ($i = 1, \dots, K$), where y_i is the label of the feature vector m_i with a value of either +1 or -1. The feature vector m lies on a hyperplane given by $w^T \cdot m + b = 0$ where w is the normal to the hyperplane. A set of feature vectors said to be optimally separated if no errors occur and the distance between closest vectors to the hyperplane is maximized. The distance $d(w, b; m)$ of a feature vector m from the hyperplane (w, b) is $d(w, b; m) = |w^T \cdot m + b| / \|w\|$. The optimal hyperplane is obtained by maximizing this margin. Multiclass SVMs can be implemented by combining several two-class SVMs. In this paper we have used both two-class SVMs and multiclass SVMs. There are a number of available implementations of SVM. We have used the freely available LibSVM (Chang and Lin, 2001) package.

5.2. Feature selection procedure

The SFFS method analyzes the features in ensembles and goes through cycles of elimination of redundant ones and enrollment of new ones. Pudil et al. (1994) claim that the best feature set is constructed by adding to and/or by removing from current set of features until there no more performance improvement is possible. SFFS algorithm can be briefly described as follows.

1. Choose from the set of K features the best two features; i.e., the pair yielding the best classification result.
2. Add the most significant feature from those remaining, where the selection is made on the basis of the feature that contributes most to the classification result when all are considered together.
3. Determine the least significant feature from the selected set by conditionally removing features one by one, while checking whether the removal of any feature improves or reduces the classification result. If it improves, remove this feature and repeat step 3 for other features; otherwise, do not remove this feature and go to step 2.
4. Stop when the number of selected features equals the number of features required.

In each step SVM classifiers are used to test the performance of the selected feature set.

5.3. Experimental results for source camera-model identification

5.3.1. Same scene multiclass camera-model identification

In this part of experiments, we considered five distinct camera-models: Canon Powershot A80, Datron DC4300, HP Photosmart 635, Kodak Easyshare LS420 and Sony DSC-P72 with image sizes 1024×768 , 1280×960 , 1600×1200 , 1752×1168 , and 1280×960 , respectively. For each camera, we captured 200 images at default settings. As exemplified in Fig. 5, the pictures were taken from the same scene. This ensures that camera properties are not detected based on textural attributes of the scenery. Half of the images were used for training in building the classifier. Then the previously unseen half of the images is used for testing the designed classifiers.

We first designed a classifier for discriminating four cameras: Canon, Datron, HP and Sony. The accuracy is measured as 88% and corresponding confusion matrix is given in Table 1. We also designed a classifier considering five camera-models. In this case, detection accuracy is measured to be 84.8%, and the corresponding confusion matrix is provided in Table 2. We can conclude from Table 3 that Kodak and Canon camera-models are likely to use similar interpolation algorithms for demosaicing as they are misclassified among each other.

5.3.2. Different scene multiclass camera-model identification

In the second part of the experiments, to evaluate the reliability of features in identification of different camera-models, we collected images taken under independent circumstance that includes various different scenes. We have considered three different cameras. These cameras include a Sony DSC 90, a Sony DSC-P72 and a Canon Powershot S1 IS. The images in all sets are in JPEG format and are of sizes 1728×2304 , 960×1280 , and 1536×2048 , respectively. In this case, we obtained 600 images from each camera and used half of them for training our classifier and the other half for testing purposes. When classifiers are designed to distinguish between all possible pairs, the accuracies of the classifiers are measured as 100% in all cases. In the case of identifying the source camera-model among three cameras, the accuracy of the classifier is measured to be 92.56% with confusion matrix as given in Table 3. We also provide scatter plots in Fig. 6 to show how well we can discriminate these cameras. Fig. 6a and b displays scattering of two features obtained from Sony P72&Sony S90 and Sony S90&Canon S1, respectively. Similarly, in Fig. 6c scatter plot for three features are given. In all figures the cameras are separated into clusters very well.

5.3.3. Different scene two-class camera-model identification

In this set, rather than trying to classify the structure of artifacts, we determine if the artifacts exhibit a specific structure. In our experiments we deployed the images taken by three cameras in Section 5.3.2. For this setup we considered 600 images from each camera. We also collected 5300 images captured by various models of different digital cameras. For each camera-model we designed different classifiers so that



Fig. 5 – Sample set of pictures taken by five camera-models. (a) Canon Powershot A80 (b) Datron DC4300 (c) HP Photosmart 635 (d) Kodak Easyshare LS420 (e) Sony Cybershot DSC-P72.

Table 1 – Confusion table for four cameras

		Predicted			
		Canon	Datron	HP	Sony
Actual	Canon	84	7	2	6
	Datron	4	87	1	3
	HP	9	6	93	3
	Sony	3	0	4	88

Table 2 – Confusion table for five cameras

		Predicted				
		Canon	Datron	HP	Kodak	Sony
Actual	Canon	73	6	0	10	8
	Datron	4	88	0	3	1
	HP	0	0	96	4	1
	Kodak	16	4	2	78	5
	Sony	7	2	2	5	85

Table 3 – Confusion table for three cameras (with the images of different scenes)

		Predicted		
		Sony P72	Sony S90	Canon S1
Actual	Sony P72	258	10	32
	Sony S90	8	289	3
	Canon S1	10	4	286

our classifier would decide if the image is from that particular camera-model or not. We used 300 images from each camera-model and 300 images from the mixed set to train the classifiers. The remaining 300 + 5000 images are used for the testing the resulting classifier. The corresponding results are presented in Table 4.

5.4. Results for combination of demosaicing characteristics with sensor noise properties

In this part of the experiment, our aim is to determine whether or not an image is captured by a particular camera. For this

Table 4 – Results for three camera-models against the mixed set

Camera-Model	Accuracy (%)
Sony P72	83.94
Sony S90	90.71
Canon S1	90.96

purpose, first we applied the method described in Lukáš et al. (2006). Afterwards we tested combination of this method with the class characteristics. We used the same dataset of Section 5.3.3. For each camera we used first 300 images to extract the sensor noise and also to design the classifier based on demosaicing artifacts. For the classifier design we used 300 training images from the mixed set as well. Remaining 300 images from the cameras and 5000 images from the mixed set is used for testing. Fig. 7 shows the accuracies we obtained with sensor noise based method and the combined procedure.

In these figures, y-axes indicate accuracy, which is defined as the ratio of the number of correct decisions to overall number of decisions. For example, when the decision threshold for sensor pattern noise based detection scheme is

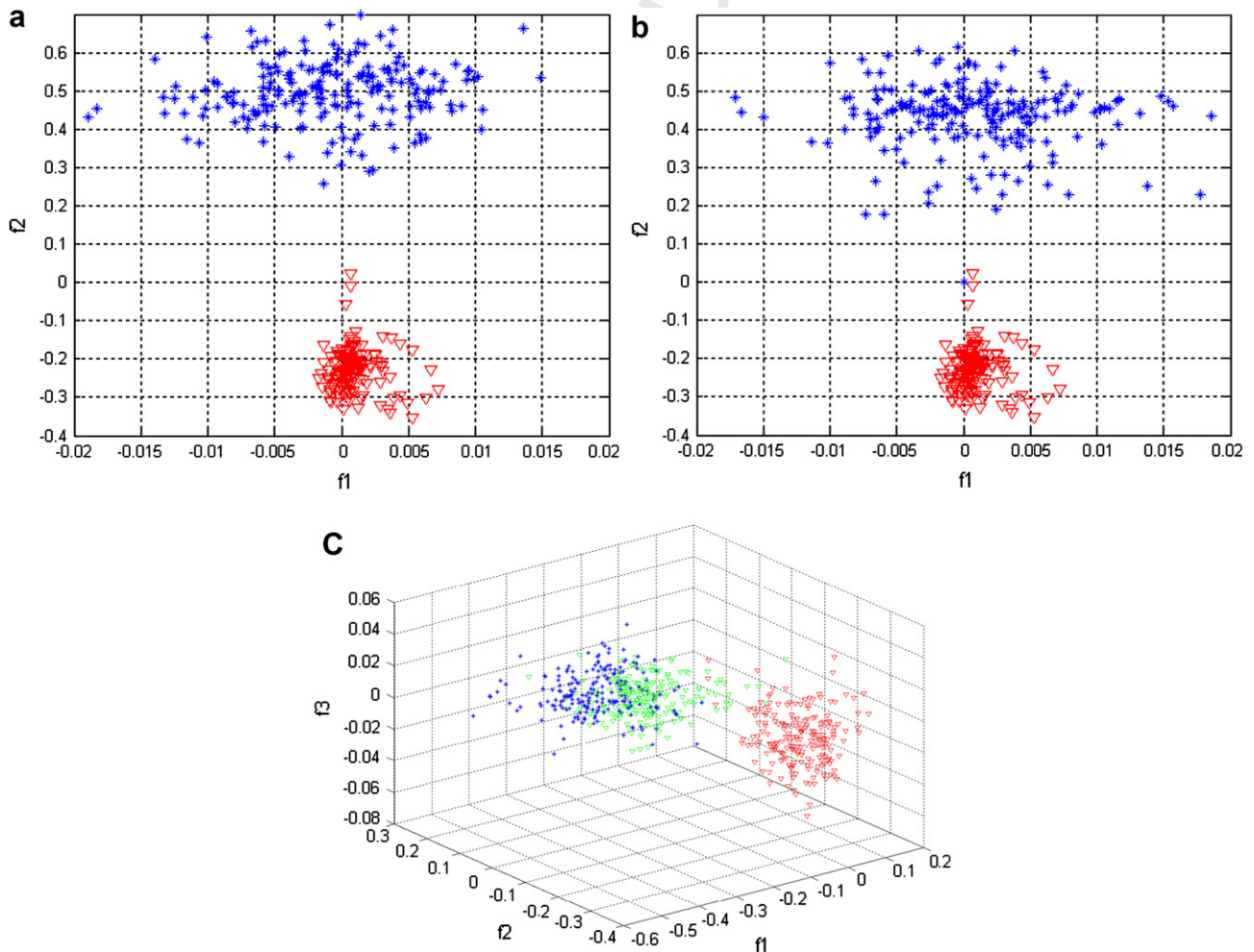


Fig. 6 – The scatter diagrams of features (a) Sony P72 and Sony S90 (b) Sony S90 and Canon S1 (c) Sony P72, Sony S90 and Canon S1.

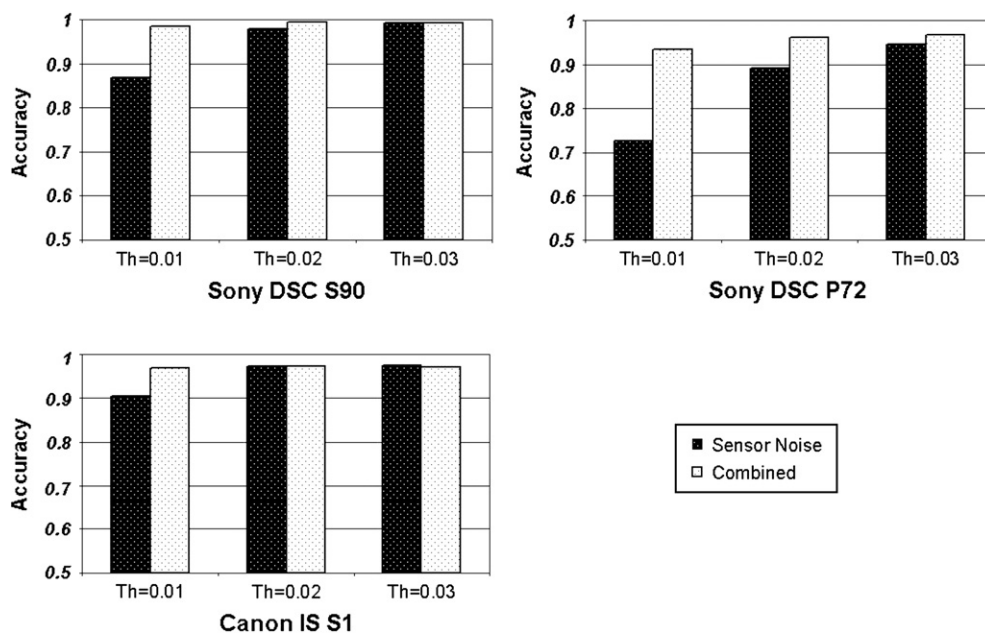


Fig. 7 – Performance comparison for three different cameras.

set to 0.01, with the combined method the accuracy improves from 72.58% to 93.41% for Sony DSC-P72. Our results show that the combined decision process yields better results by reducing the false-positive considerably while the reduction of true positives is rather low.

6. Discussion

In this work, we describe a method to differentiate different digital camera-models based on demosaicing artifacts. We design our classifiers using images taken from the same scene and under similar settings as well as the images taken under independent conditions with no relation to each other. In these experiments, the accuracy results for identifying up to five camera-models are measured to be approximately 90%. According to these results we can conclude that even if the scene and camera settings are the same demosaicing artifacts can be used to detect and classify interpolation algorithms used by different camera-models. In order to provide more realistic results we design classifiers which discriminate a single camera-model from a very large number of camera-models. In this case we obtained approximately 90% accuracy as well. Furthermore, we described a new scheme for individual source camera identification by adding a new layer of verification through requiring camera-model properties are in agreement with individual camera properties. For this purpose, we incorporate our proposed method with the sensor noise based camera identification method of Lukáš et al. (2006) and show that the accuracy can be improved by an average of 6%. An open problem in image forensics is the robustness of the proposed techniques to malicious processing. Our current research focuses on designing methods that can resist and detect malicious processing.

REFERENCES

- Bayram S, Sencar HT, Memon N. Source camera identification based on CFA interpolation. In: Proceedings of IEEE ICIP; 2005.
- Bayram S, Sencar HT, Memon N, Avci I. Improvements on source camera-model identification based on CFA interpolation. In: Proceedings of WG 11.9 international conference on digital forensics; 2006.
- Bayram S, Avci I, Sankur B, Memon N. Image manipulation detection. *Journal of Electronic Imaging* October–December 2006;4.
- Chang C, Lin C. LIBSVM: a library for support vector machines; 2001. Software available at: <http://www.csie.ntu.edu.tw/~cjlin/libsvm>.
- Chen M, Fridrich J, Goljan M, Lukáš J. Source digital camcorder identification using sensor photo response non-uniformity, Security, steganography, and watermarking of multimedia contents IX. In: Proceedings of the SPIE, vol. 6505; 2007. pp. 65051G.
- Chen M, Fridrich J, Goljan M. Digital imaging sensor identification (further study), Security, steganography, and watermarking of multimedia contents IX. In: Proceedings of the SPIE, vol. 6505; February 2007. pp. 65050P.
- Choi KS, Lam EY, Wong KKY. Source camera identification using footprints from lens aberration, *Digital photography II*. In: Proceedings of the SPIE, vol. 6069; February 2006. 172–179.
- Dehnie S, Sencar HT, Memon N. Identification of computer generated and digital camera images for digital image forensics. In: Proceedings of IEEE ICIP; 2006.
- Dirik E, Bayram S, Sencar HT, Memon N. New features to identify computer generated images. In: Proceedings of IEEE ICIP; 2007.
- Dirik AE, Sencar TH, Nasir M. Source camera identification based on sensor dust characteristics. In: IEEE workshop on signal processing applications for public security and forensics, SAFE '07; April 2007.
- Gallagher AC. Detection of linear and cubic interpolation in JPEG compressed images. In: Proceedings of CRV; 2005.
- Geradts ZJ, Bijhold J, Kieft M, Kurusawa K, Kuroki K, Saitoh N. Methods for identification of images acquired with digital cameras. *Proceedings of SPIE* 2001;4232.

- 1141 Gunturk BK, Glotzbach J, Altunbasak Y, Schafer RW, 1171
1142 Mersereau RM. Demosaicking: color filter array interpolation 1172
1143 in single chip digital cameras. *IEEE Signal Processing Magazine* 1173
1144 September 2004;9. 1174
1145 Johnson M, Farid H. Exposing digital forgeries by detecting 1175
1146 inconsistencies in lighting. In: *ACM multimedia and security* 1176
1147 *workshop*; 2005. 1177
1148 Kharrazi M, Sencar HT, Memon N. Blind source camera 1178
1149 identification. In: *IEEE international conference on image* 1179
1150 *processing*, vol. 1; October 2004. 709–712. 1180
1151 Kurosawa K, Kuroki K, Saitoh N. CCD fingerprint method – 1181
1152 identification of a video camera from videotaped images. 1182
1153 In: *ICIP' 99*, Kobe, Japan; 1999. 1183
1154 Long Y, Huang Y. Image based source camera identification using 1184
1155 demosaicking. In: *IEEE 8th workshop on multimedia signal* 1185
1156 *processing*, Victoria, BC; October 2006; pp. 4190–424. 1186
1157 Lukáš J, Fridrich J, Goljan M. Digital camera identification from 1187
1158 sensor noise. *IEEE Transactions on Information Security and* 1188
1159 *Forensics* June 2006;1:205–14. 1189
1160 Moon Todd. The expectation maximization algorithm. *IEEE Signal* 1190
1161 *Processing Magazine* 1996. 1191
1162 Ng Tian-Tson, Chang Shih-Fu, Lin Ching-Yung, Sun Qibin. 1192
1163 Passive-blind image forensics. In: Zeng W, Yu H, Lin Ching- 1193
1164 Yung, editors. *Multimedia security technologies for digital* 1194
1165 *rights*. Elsevier; 2006. 1195
1166 Popescu A, Farid H. Exposing digital forgeries by detecting traces 1196
1167 of re-sampling. *IEEE Transactions on Signal Processing* 2004. 1197
1168 Popescu A, Farid H. Exposing digital forgeries in color filter array 1198
1169 interpolated images. *IEEE Transactions on Signal Processing* 1199
1170 2005;53(10):3948–59. 1200
- Pudil P, Ferri FJ, Novovicov J, Kittler J. Floating search methods 1171
for feature selection with nonmonotonic criterion 1172
functions. In: *Proceedings of the 12th ICPR*, vol. 2; 1994. 1173
279–283. 1174
- Sencar HT, Memon N. Overview of state-of-the-art in digital 1175
image forensics, Indian Statistical Institute platinum jubilee 1176
monograph series titled statistical science and 1177
interdisciplinary research. World Scientific Press; 2008. 1178
- Sutcu Y, Bayram S, Sencar HT, Memon N. Improvements on 1179
sensor noise based source camera identification. In: 1180
Proceedings of IEEE ICME; 2007. 1181
- Swaminathan A, Wu M, Ray Liu KJ. Image tampering 1182
identification using blind deconvolution. In: *Proceedings of* 1183
the IEEE international conference on image processing (ICIP); 1184
2006. p. 2311–4. 1185
- Swaminathan A, Wu M, Ray Liu KJ. Non intrusive forensic 1186
analysis of visual sensors using output images. *IEEE* 1187
Transactions of Information Forensics and Security March 1188
2007;2(1):91–106. 1189
- Tian-Tsong N, Shih-Fu C, Yu-Feng H, Lexing X, Mao-Pei T. 1190
Physics-motivated features for distinguishing photographic 1191
images and computer graphics. Singapore: *ACM Multimedia*; 1192
November 2005. 1193
- Tran Van Lanh, Kai-Sen Chong, Sabu Emmanuel, Kankanhalli MS. 1194
A survey on digital camera image forensic methods. In: 2007 1195
IEEE international conference on multimedia and expo; 2007. 1196
- Wang Y, Moulin P. On discrimination between photorealistic and 1197
photographic images. In: *IEEE international conference on* 1198
acoustics, speech and signal processing, vol. 2. *IEEE*; May 2006. 1199
II-161–II-164. 1200